MASSACHUSETTS INSTITUTE OF TECHNOLOGY
ARTIFICIAL INTELLIGENCE LABORATORY

Working Paper 337 July, 1992

Tomorrow's Surgery: Micromotors and Microrobots

Anita M. Flynn
MIT Artificial Intelligence Laboratory

K.R. Udayakumar
Penn State Materials Research Laboratory,

David S. Barrett
MIT Ocean Engineering Department

Abstract

Surgical procedures have changed radically over the last few years due to the arrival of new technology. What will technology bring us in the future?

This paper examines a few of the forces whose timing are causing new ideas to congeal from the fields of artificial intelligence, robotics, micromachining and smart materials.

Intelligence systems for autonomous mobile robots can now enable simple insect level behaviors in small amounts of silicon. These software breakthroughs coupled with new techniques for microfabricating miniature sensors and actuators from both silicon and ferroelectric families of materials offer glimpses of the future where robots will be small, cheap and potentially very useful to surgeons.

In this paper we relate our recent efforts to fabricate piezoelectric micromotors in an effort to develop actuator technologies where brawn matches to the scale of the brain. We discuss our experiments with thin film ferroelectric motors $2mm$ in diameter and larger $8mm$ versions machined from bulk ceramic and sketch possible applications in the surgical field.

1 Intelligent Machines

Today surgeons routinely remove organs with minimally invasive procedures that were unheard of just a few years ago. What will be next?

It seems clear that more dextrous manipulators and better visualization tools will be the upcoming items on the agenda. After that, perhaps placing the intelligence also at the point of interest? While the idea of an autonomous robot running amuck inside the human body is a scary thought, it certainly is plausible to imagine beginning with low level reflexive actions for locomotion or manipulation carried out autonomously, while a fiber-optic cable is tethered to a surgeon for observation and direction.

At the MIT Mobile Robotics Laboratory, new approaches in artificial intelligence have led to novel intelligence architectures used on robots which explore, build maps, have an onboard manipulator, walk, interact with people, navigate visually and learn to coordinate many conflicting internal behaviors [1]. This type of control system, known as a subsumption architecture, is implemented as a distributed layered network of augmented message-passing finite state machines [2] and enables very tight loops between perception and action to be maintained in a mobile robot's dynamically changing world.

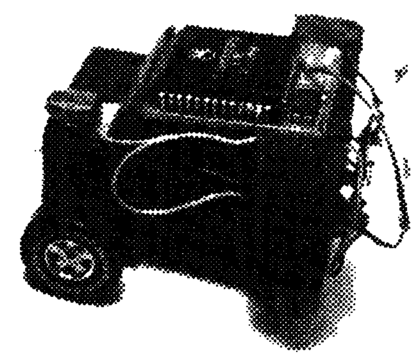

Figure 1: Squirt is an autonomous robot measuring 2.5*cm* on a side, carrying onboard computer, sensors, motor and batteries.

Figure 1 illustrates Squirt, the smallest simplest robot built under this paradigm [3]. Two microphones and a light sensor trigger insect style behaviors of hiding in the dark and moving towards noise. The subsumption program endowing Squirt with these capabilities fits in a very lean 1300 bytes of code.

Unfortunately, Squirt's lone DC gearhead motor grants only one degree of freedom; forwards or back and turn (when a clutch on the rear axle allows one wheel to slip). While an entire computer with accompanying software, sensors and batteries can fit into a Squirt-sized package, it is difficult to include very many motors for finer dexterity.

With the advent of silicon micromachining techniques in which electrostatic motors the size of a human hair can be etched in place on the surface of a silicon chip [4], the thought arose to pattern an entire robot on a chip [5]; sensors, subsumption control system compiled to the gate level, actuators and solar cells, as all components could be fabricated in silicon. Resulting machines could be printed in the same manner as integrated circuits and mass produced in low cost batch fabrication lots, enabling *cheap disposable robots.*

Unfortunately, the problem here is that silicon electrostatic motors have a number of drawbacks for small robots. They typically spin at high speeds with very small torque and are hard to scale up, necessitating that the rest of the system be scaled down to their domain.

We would be interested in slightly larger, but still small motors which would be compact, direct-drive, cost-effective and able to couple useful torque to a load for the purpose of creating robots that act as autonomous sensors and manage to find their way into hard to reach places.

A number of technologies look promising here such as magnetic or electrostatic wobble motors [6], polymer gels for artificial muscles [7] and piezoelectric ultrasonic motors [8]. Our investigations are focused on scaling down ultrasonic motors and attempting to microfabricate them using new ferroelectric thin films of lead zirconate titanate (PZT) [9].

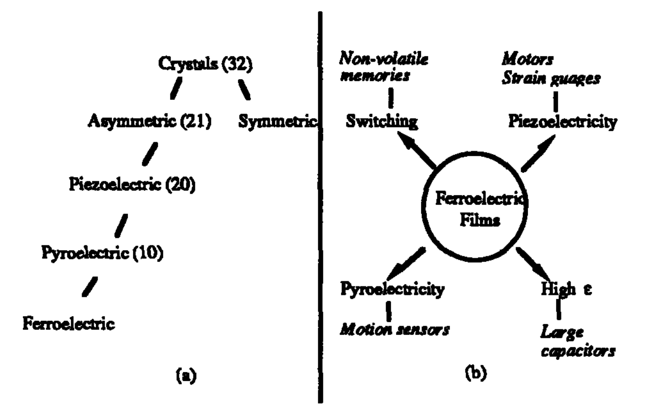

Figure 2: (a) Subsets of assymetric crystal classes exhibit the effects of piezoelectricity, pyroelectricity and ferroelectricity. (b) These effects can be used to create capacitors, memories, sensors and actuators.

1.1 Smart Materials

Figure 2 illustrates why we find stepping outside the bounds of traditional silicon microprocessing and adding thin film PZT to be intriguing for microfabricated robots. While ferroelectric materials such as PZT have high dielectric coefficients ($\epsilon = 1300\epsilon_o$) and a hysteretic relationship between polarization and electric field making them excellent materials for capacitors and non-volatile memories, ferroelectrics also exhibit pyroelectric and piezoelectric effects. The pyroelectric effect is a change in charge density when the material is uniformly heated and the piezoelectric effect is a similar response when the material is stressed. The pyroelectric and piezoelectric effects can be utilized to create infrared and force sensors. The piezoelectric effect can be applied in the reverse manner where an applied voltage induces the material to deform. This latter characteristic is the basis of piezoelectric actuators. Thus many components of a robot can be fabricated with the addition of this one material to a traditional silicon process.

1.2 The Piezoelectric Effect

Piezoelectricity describes the first order (linear) coupling between the dielectric and elastic phenomena. For an anisotropic, homogeneous solid, under isothermal conditions, and negelecting the magnetic field effects, the components of the elastic strain tensor x_{ij} are given by the following relation:

$$x_{ij} = s^E_{ijkl} X_{kl} + d_{ijk} E_k + \text{ higher order terms}$$

where X_{kl} and E_k are the components of the stress tensor and the electric field vector, respectively. The s^E_{ijkl} coefficients are the components of the elastic compliance tensor measured at constant electric field. The components d_{ijk} of the piezoelectric tensor define the electromechanical coupling. Neglecting higher order terms, if a static electric field is applied to a piezoelectric material that is free to change shape, the total stress X is zero and the equation reduces to $x_{ij} = d_{ijk} E_k$. The piezoelectric term thus relates the mechanical strain developed in a material as a consequence of the electric field applied to the material. d is thus called the strain coefficient, and the equation defines the converse piezoelectric effect. Alternatively, for a linear, anisotropic, homogeneous, polarizable solid, the components of the dielectric displacement vector D_i are given by the relation:

$$D_i = d_{ijk} X_{jk} + \epsilon^X_{ij} E_j + \text{ higher order terms}$$

where ϵ^X_{ij} are the components of the dielectric permittivity tensor measured at constant stress. Again, neglecting higher order terms, if a stress is applied to the piezoelectric material that is short-circuited, the total electric field across the material is zero, and the equation above becomes $D_i = d_{ijk} X_{jk}$. In this case, the piezoelectric term relates the charge developed on the material's surface upon application of stress. The d coefficient is then called the piezoelectric charge coeffiecient and the corresponding electromechanical coupling is known as the direct piezoelectric effect.

1.3 Motors

Figure 3 is a photograph of a $2mm$ thin film PZT micromotor structure fabricated on a $1\mu m$ thick silicon nitride membrane. A small plano-convex glass lens placed down upon the substrate is used as the rotor and spins at 100–300rpm for $90kHz$ excitation at $5V$ [10, 11].

These initial structures validated the films as useful for actuators but did not incorporate any bearings or means for coupling power out. Larger

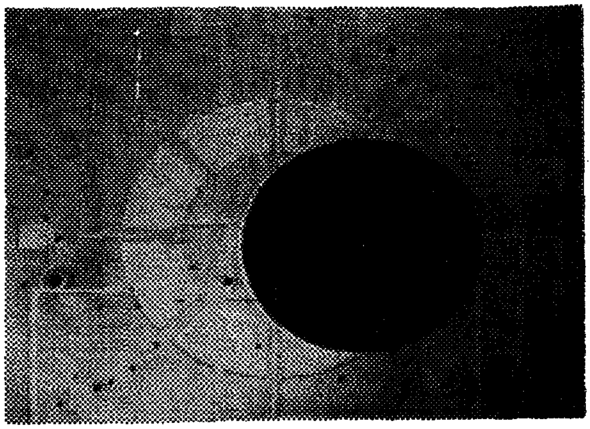

Figure 3: Thin film PZT is used to fabricate piezoelectric micromotors.

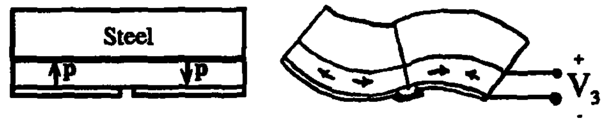

Figure 4: Neighboring electroded segments if alternately poled will strain oppositely when driven with a common voltage.

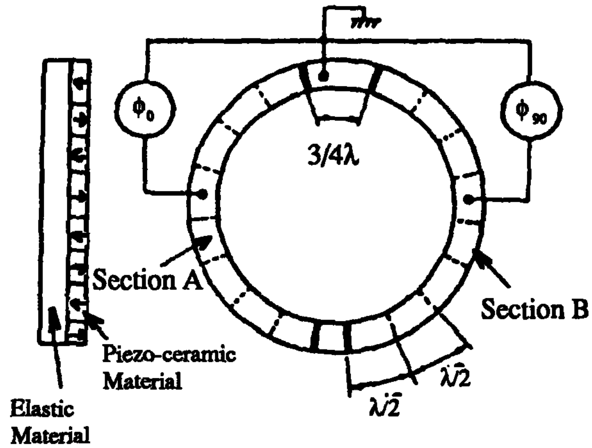

Figure 5: Two standing wave offset by $\frac{\lambda}{4}$ and driven 90 degrees out of phase combine to form a traveling wave of deformation.

ultrasonic motors which are commercially popular in Japan [12, 13, 14] use bulk ceramic PZT in an annular ring configuration as shown in figure 5. Figure 4 illustrates the basic principles behind a ring-type ultrasonic motor. Bulk ceramic PZT is bonded in segments onto an elastic body such as steel. A large electric field is applied to each segment oppositely to induce an initial polarization direction. When all segments are wired together and driven with a common voltage, neighboring segments strain in opposing directions causing the structure to buckle. An oscillating applied voltage converts the buckle pattern into a standing wave of mechanical deformation.

Ring-type ultrasonic motors superimpose two standing waves which are a quarter wavelength out of phase in both space and time (figure 5) to generate a traveling wave of bending. A traveling wave has the property that any point on the surface of the beam moves in an elliptical trajectory perpendicular to the plane of the ring. A rotor pressed against the surface is then propelled along through friction. These types of motors consequently generate high torque at low speeds and do not require gears.

Presently, we are experimenting with smaller versions of bulk ceramic ultrasonic motors, but which are larger than the thin film structures on membranes. Figure 6 shows a stator of an ultrasonic motor $8mm$ in diameter.

While bulk ceramic PZT requires high voltages (typically 50–100V) to achieve the required field strengths, thin film PZT is 500 times thinner and can run directly from batteries without recourse to DC-DC converters. Since the motors can also perform without gears in a direct-drive fashion, significant weight can be reduced for a mobile robot. Figure 7 shows our thin film PZT stators, of the same dimensions as the ring-type stator of figure 6, which have been microfabricated in a new laser-based process which requires zero masks and no wet etching, offering potential for low cost fabrication.

2 Mini Robots

If small compact useful motors were available, what kinds of systems could we build and what orders of speeds and torques would we require? Essentially, we would like motors of the same size scale as the sensors we use today. This is especially true for

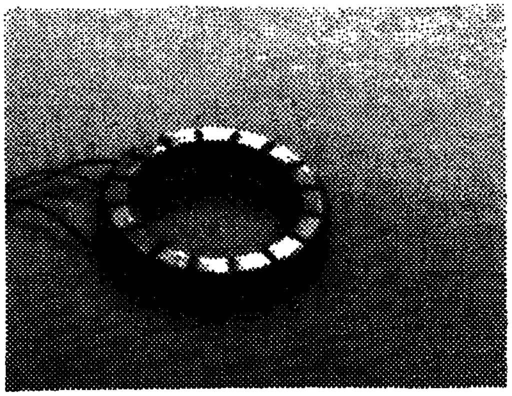

Figure 6: The stator of an $8mm$ ultrasonic motor is made from bulk ceramic PZT bonded onto a ring of steel.

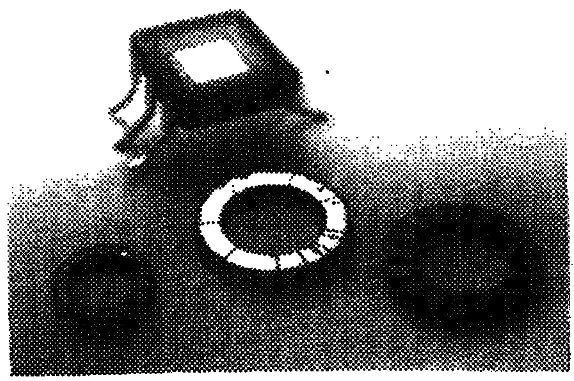

Figure 7: Laser processed ultrasonic motor stators are comprised of layers of oxide, titanium, platinum, PZT and gold, on a silcon substrate.

robots whose job is to collect information as opposed to heavy-lift assembly operations. We now sketch a number of plausible systems.

2.1 A One Cubic Centimeter Camera-Toting Cart

Using the strategy of batch fabricating half a motor and hand assembling the rest, with $8mm$ motors it is conceivable to build a very useful system, a small teleoperated robot propelling a camera. On earlier robots we have used 192×165 serial CCD imagers in 6-pin packages (manufactured by Texas Instruments and shown in figure 7). This camera would be roughly the same size as our motor.

We propose to use two small direct drive $8mm$ motors surface-mounted onto a flexible printed circuit board which bends to form the chassis of the cart as shown in figure 8. Small rubber O-rings are pushed onto the rotor and serve as tires for the piezomotor-driven wheels. Wires run from the stators to a connector for the tether. The camera chip and small lens mount on a top flap of the flex printed circuit and a castor on the bottom provides a three-point stance. The entire package should fit in roughly one cubic centimeter and will contain twice as many degrees of freedom as Squirt.

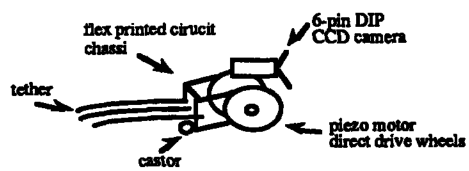

Figure 8: Two $8mm$ piezomotors with rubber O-rings wrapped around the rotors could serve as tires for a two-degree-of-freedom steerable cart.

2.2 Micro Crawlers

Other means of locomotion besides wheels can be useful for microrobots. Here is a simple design and torque requirements for a six legged walker incorporating twelve piezoelectric micromotors (figure 9).

Each hip contains two motors marked α and β, (for advance and balance respectively). The robot walks in a tripod gate with power coming from off-board via a tether. The β motors must be able to support $\frac{1}{3}$ the total bug weight and lift the leg clear of the ground. The α motors carry a much lighter load, and so the same β motor design will suffice. What sorts of torques and power supplies are required here? Table I lists dimensions and materials for one specific bug design.

Table I. Bug parameters and torque requirements.

Body	$2.5cm \times 6.4mm \times 3.2mm$
(Aluminum)	$\rho =$ density $= 2706\frac{kg}{m^3}$
Motors	$3.2mm$ dia.$\times 3.2mm$ long

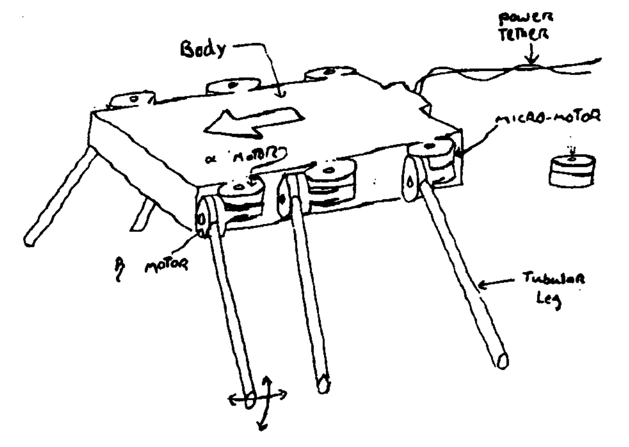

Figure 9: The high torque, low speed characteristic of a piezomotor means that it can be used in a direct drive fashion which is convenient for robots, especially those with many degrees of freedom such as this six-legged walker.

(Silicon)	$\rho =$ density $= 2596\frac{kg}{m^3}$
Legs	$1.3mm$ dia.$\times 9.5mm$ long
(Steel)	$\rho =$ density $= 7731\frac{kg}{m^3}$
Leg weight	$0.9g$
Total weight	$2.07g$
Torque – support	$4.6 \times 10^{-4} kgf\text{–}cm$
Torque – lifting	$4.5 \times 10^{-5} kgf\text{–}cm$
Power – lifting $\frac{1rad}{s}$	$4.5 \times 10^{-5} W/motor$
Power – total	$1.35 \times 10^{-4} W$
Current at $5V$	$2.7 \times 10^{-5} A$

In a tripod gate, three legs are in the air at any one time. Total weight includes the body, six motors and three legs. The maximum torque required for each of the three motors to support one third of the total body weight is calculated as the legs touch the ground at a 45 degree angle from the body. Power requirements per motor are calculated as though providing this torque at the rate of one radian per second. Table I then gives us some feeling for the ballpark torques and power supplies a small robot might require. In this case, required torque is $4.6 \times 10^{-4} kgf\text{–}cm$.

2.3 Micro Submersibles

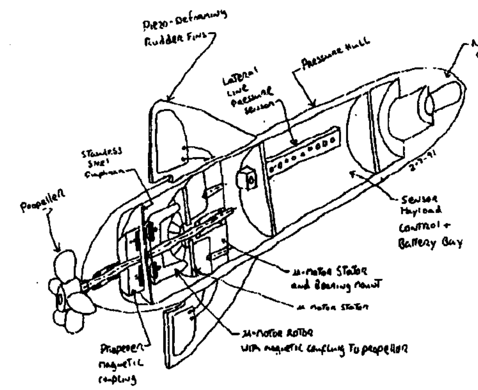

Figure 10: A $2.5cm$ long submarine robot incorporates a piezoelectric micromotor for propulsion.

An underwater robot's propulsion system might be similar to that portrayed in figure 10. A floating or submersible robot would be quite a bit easier to build than a walker because a neutrally buoyant swimmer can carry weight equivalent to the weight of the water it displaces.

In order to calculate the types of torques a small submarine would need let us assume the submarine is cylindrically shaped with a diameter of $5mm$ and a length from nose to end of $25mm$. We will also assume that the motor is cylindrically shaped $4mm$ in diameter and $3mm$ long.

$$D_s = 5mm$$
$$L_s = 25mm$$
$$\rho_w = \text{density of water} = 998\frac{kg}{m^3}$$
$$\nu_w = \text{viscosity} = 1.0 \times 10^{-6}\frac{m^2}{\text{sec}}$$
$$D_m = 4mm$$
$$L_m = 3mm$$
$$\rho_{si} = \text{density of silicon} = 2340\frac{kg}{m^3}$$

Weight of water displaced $= \frac{\pi D_s^2}{4} L_s \rho_w = 0.49g$
Weight of the motor $= \frac{\pi D_m^2}{4} L_m \rho_{si} = 0.088g$
Weight of payload allowed $= 0.402g$

The drag force in the water is a function of the coefficient of drag, the density of the water, the velocity of the submarine and its cross-sectional area.

$$D_F = C_d \left(\frac{\rho_w V^2 A}{2}\right)$$

$$C_d = \text{coef drag} = 0.44\frac{D_s}{L_s} + 0.16\frac{L_s}{D_s} + 0.016\sqrt{\frac{D_s}{L_s}}$$

$$\text{where } 1 \leq \frac{L_s}{D_s} \leq 10 \qquad \text{Re} \leq 2 \times 10^5 \quad \text{Re} = \frac{VD_s}{\nu_w}$$

Let us assume a velocity of the submarine of $V = 10\frac{mm}{\text{sec}}$.

$D_F = 1.72 \times 10^{-7}N$
Re = 10 (regime is correct for coeff. of drag)

Now we calculate the thrust produced by the propeller. For steady state translation, the thrust must just offset the drag. Assume a propeller diameter of $5mm$.

d = diameter of propeller = $5mm$
Q = shaft torque
T = axial thrust
N = angular velocity of propeller
V = free stream velocity
P = propeller pitch
J = advance ratio $\frac{V}{Nd}$
η_p= propeller efficiency = $\frac{VT}{2\pi NQ}$
$\frac{P}{d}$ = propeller pitch to diameter ratio

For steady state translation, $T = D_F$.

$$\eta_p = \frac{VD_F}{2\pi NQ}$$

$$Q = \frac{VD_F}{2\pi N\eta_p}$$

Assuming that the propeller turns at $N = 100rpm$, the advance ratio J is approximately 0.2. Propeller characteristics are given in terms of propeller efficiency vs. advance ratio for a given propeller pitch to diameter ratio. For this advance ratio and a $\frac{P}{d}$ of 0.6, η_p is known to be 0.2. Now we can calculate the shaft torque and motor power.

$Q = 1.3 \times 10^{-10}Nm = 1.3 \times 10^{-9}kgf\text{-}cm$
$P_m = Q \times N = \text{motor power} = 1.4 \times 10^{-9}W$

This tells us that the torques and power requirements for neutrally bouyant systems can be quite small. This is good news for medicine, because robotics for fluid filled tubes in the human body is just ocean engineering on a tiny scale.

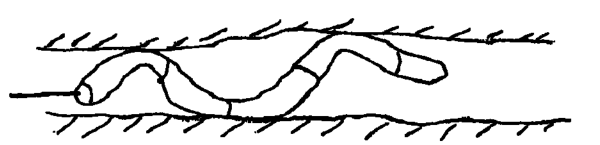

Figure 11: A crawling robot wiggles its way down a tube using a traveling wave of bending.

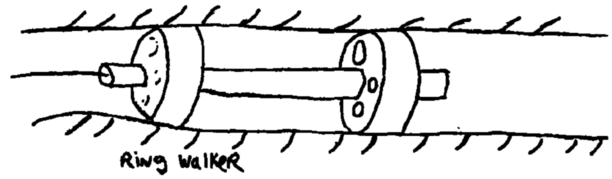

Figure 12: This ring-walker is a piezoelectric inchworm drive which alternately locks, contracts and extends each end.

3 The Future

A revolution has occurred in surgery in the last few years but the best is yet to come. Laparoscopic and endoscopic tools extend the doctor's hands and eyes, but for the most part the surgeon plays the part of the solo performer in a quartet. Perhaps in the future, his or her role will be that of a conductor of an orchestra, where a team of micro interns find their way through the maze of tubes in the body, carrying sensors and tools and freeing the surgeon of the taxing burden of negotiating every low level activity.

3.1 Micro Interns

With a team of intern robots, the surgeon can have access to parallel mechanical systems under supervisory control where the supervisor and interns work in a master-slave fashion over a fiber optic or radio link tether. Once this level of teleoperated surgery is established, it is a simple conceptual leap to splicing the tether to geographically dispersed experts around the globe. Thus the right thumb expert in New York or the left toe expert in Bordeaux can help the same patient in Antarctica.

Micromotors and microrobots have high potential in a number of medical procedures. From the GI tract to the vascular system, autonomous ma-

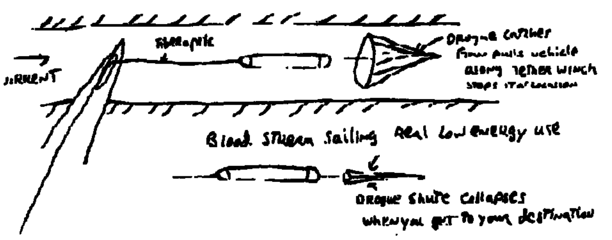

Figure 13: An umbrella-bot sails down the bloodstream reeling out a tether which is locked once the robot reaches the point of interest.

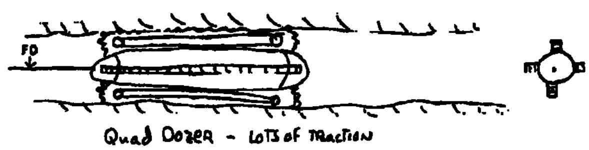

Figure 14: This quad-dozer trundles through pipes while gripping with four tank treads.

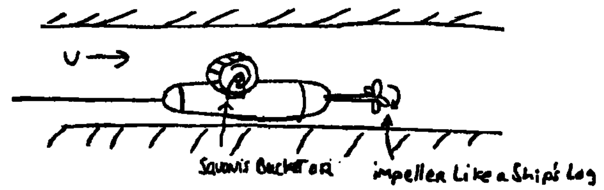

Figure 15: A turbine generates power from the energy supplied by rushing currents.

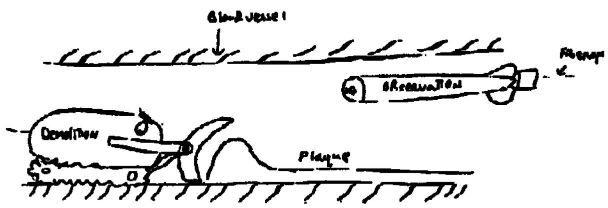

Figure 16: This demolition-bot scrubs away at congesting placque.

chines could act as drug delivery systems, roto-rooters, grinders, markers, artificial sphincters, auxiliary pumps, valves, self-cleaning filters, mobile dams or autonomous endoscopes. Chemical sensors, pressure sensors and flow sensors are now routinely made on silicon microchips and so a little bit of sensing, a little bit of intelligence and a little bit of actuation could be arranged to implement implants that monitor and control flows of various sorts.

What will these medical microrobots look like? Figures 11- 14 depict some possible propulsion systems. Manuevering down a tube might be achieved by a traveling wave crawler as shown in figure 11 or as a piezoelectric inchworm (figure 12) which alternately locks, extends and contracts to inch its way down a pipe. A form of sailing might propel an umbrella-laden robot along a blood vessel (illustrated in figure 13), using the flow to push it along and dragging a tether which could be winched in to hold it in place once it has reached its destination. For more rugged terrain, four tank treads equally located around the cylindrical body of a microrobot would find traction by grasping onto the side walls, as shown in figure 14. For power, miniature batteries could be placed onboard, energy could be supplied through a tether, or perhaps a paddle-wheel generator would tap into the rushing currents as sketched in figure 15. For cleaning tasks, the demolition-bot shown in figure 16 would use a simple manipulator for clearing debris.

A revolution has occurred in surgery in the last few years, but the fun has only just begun.

4 References

[1] Rodney A. Brooks, "New Approaches to Robotics", *Science*, vol. 253, pp. 1227–1232, September 13, 1991.

[2] Rodney A. Brooks, "A Robust Layered Control System for a Mobile Robot", *IEEE Journal of Robotics and Automation*, RA-2, pp. 14–23, April, 1986.

[3] Anita M. Flynn, Rodney A. Brooks, William M. Wells III and David S. Barrett, "Intelligence for Miniature Robots", *Journal of Sensors and Actuators*, vol. 20, pp. 187–196, 1989.

[4] Roger T. Howe, Richard S. Muller, Kaigham J. Gabriel and William S. N. Trimmer, "Silicon Micromechanics: Sensors and Actuators on a Chip", *IEEE Spectrum*, pp. 29–35, July 19, 1990.

[5] Anita M. Flynn, "Gnat Robots (And How They Will Change Robotics)", *Proceedings of the IEEE Micro Robots and Teleoperators Workshop*, Hyannis, MA, November, 1987.

[6] S.C. Jacobsen, R. H. Price, J.E. Wood, T.H. Rytting and M. Rafaelof, "The Wobble Motor: An Electrostatic, Planetary Armature, Microactuator", *Proceedings of the IEEE Micro Electro Mechanical Systems Conference*, Salt Lake City, UT, pp. 17–24, February 20–22, 1989.

[7] David L. Brock, "Review of Artificial Muscle Based on Contractile Polymers", *MIT Artificial Intelligence Laboratory Memo 1330*, November, 1991.

[8] K. Ragulskis, R. Bansevicius, R. Barauskas and G. Kulvietis, *Vibromotors for Precision Microrobots*, Hemisphere Publishing Co., New York, 1988.

[9] Anita M. Flynn, Rodney A. Brooks and Lee S. Tavrow, "Twilight Zones and Cornerstones: A Gnat Robot Double Feature", *MIT Aritificial Intelligence Laboratory Memo 1126*, July, 1989.

[10] Anita M. Flynn, Lee S. Tavrow, Stephen F. Bart, Rodney A. Brooks, Daniel J. Ehrlich, K.R. Udayakumar and L. Eric Cross, "Piezoelectric Micromotors for Microrobots", *IEEE Journal of Microelectromechanical Systems*, vol. 1, no. 1, pp. 44–51, March, 1992.

[11] K.R. Udayakumar, S.F. Bart, A.M. Flynn, J. Chen, L.S. Tavrow, L.E. Cross, R.A. Brooks and D.J. Ehrlich, "Ferroelectric Thin Film Ultrasonic Micromotors", *Proceedings of the Fourth IEEE Workshop on Micro Electro Mechanical Systems*, Nara, Japan, pp. 109–113, Jan. 30–Feb. 2, 1991.

[12] Toshiiku Sashida, "Traveling Wave Ultrasonic Motors", in *Ultrasonic Motors and Actuators*, edited by Akiyama, Chapter 4, Trikepps, in Japanese, 1986.

[13] Kazuya Hosoe, "An Ultrasonic Motor for Use in Autofocus Lens Assemblies", *Techno*, pp. 36-41, in Japanese, May, 1989.

[14] Osamu Kawasaki, Takahiro Nishikura, Yoshinobu Imasaka, Masanori Sumihara, Katsu Takeda and Hiroshi Yoneno, "Ultrasonic Motors", *Denshi Tokyo*, No. 26, 1987.